

# Order parameter fluctuation and ordering competition in $\text{Ba}_{1-x}\text{K}_x\text{Fe}_2\text{As}_2$

Jing Wang,<sup>1,2</sup> Guo-Zhu Liu,<sup>1</sup> Dmitry V. Efremov,<sup>2</sup> and Jeroen van den Brink<sup>2,3</sup>

<sup>1</sup>*Department of Modern Physics, University of Science and Technology of China, Hefei, Anhui 230026, P.R. China*

<sup>2</sup>*Institute for Theoretical Solid State Physics, IFW Dresden, Helmholtzstr. 20, 01069 Dresden, Germany*

<sup>3</sup>*Institute for Theoretical Physics, TU Dresden, 01069 Dresden, Germany*

The competition among superconductivity, stripe-type magnetic order, and a unique  $C_4$  symmetric magnetic order in  $\text{Ba}_{1-x}\text{K}_x\text{Fe}_2\text{As}_2$  is theoretically studied, focusing on its influence on the global phase diagram. By carrying out a renormalization group analysis of an effective field theory, we obtain the energy-scale dependent flows of all the model parameters, and then apply the results to understand the phase diagram of  $\text{Ba}_{1-x}\text{K}_x\text{Fe}_2\text{As}_2$ . On the basis of the renormalization group analysis, we show that the critical line of nematic order has a negative slope in the superconducting dome and superconductivity is suppressed near the magnetic quantum critical point, which are both consistent with recent experiments. Moreover, we find that, although the observed  $C_4$  symmetric magnetic state could be a charge-spin density wave or a spin-vortex crystal at high temperatures, charge-spin density wave is the only stable  $C_4$  magnetic state in the low-temperature regime. This result provides a method to distinguish these two candidate  $C_4$  magnetic states.

PACS numbers: 74.70.Xa, 74.25.Ha, 74.25.Dw, 74.40.Kb, 74.62.-c

## I. INTRODUCTION

A universal property shared by most known iron-based superconductors (FeSCs) is the bulk coexistence of two or even three distinct long-range orders [1–12], such as superconductivity, stripe-type spin-density-wave (SDW) order, nematic order, and other possible orders. The competition and coexistence of these orders leads to a very complicated global phase diagram [1–12]. Acquiring a detailed knowledge of the phase diagram is an important step towards a better understanding of FeSCs.

Among the long-range orders competing with superconductivity, a particular role is played by the nematic order, induced by an electronic state that spontaneously breaks the  $C_4$  (tetragonal) symmetry of the system down to a  $C_2$  (orthogonal) symmetry. Extensive experiments have confirmed that nematic order exists in almost all FeSCs [2–5, 13–17]. In most cases, the nematic order sets in at a temperature  $T_n$  slightly higher than the critical temperature of magnetic order  $T_m$  [4, 6, 10, 18, 19]. Usually, the magnetic order is generated by a stripe-type SDW, and possesses two characteristic vectors  $\mathbf{Q}_X = (\pi, 0)$  and  $\mathbf{Q}_Y = (0, \pi)$  in the Brillouin zone of the iron square lattice, which relate to the spin operator  $S(\mathbf{r})$  in the form  $S(\mathbf{r}) = M_{X,Y} e^{i\mathbf{Q}_{X,Y}\cdot\mathbf{r}}$  [12, 55]. This stripe SDW breaks the discrete lattice rotational symmetry by selecting out only one of the two characteristic vectors  $\mathbf{Q}_X$  and  $\mathbf{Q}_Y$ , preserving the  $C_2$  symmetry [6, 8, 10, 12]. Because the nematic order and SDW order coexist over a large part of the global phase diagram, it is widely believed [3–6, 8–12] that the nematic order is actually induced by the fluctuation of magnetic order.

It came as a surprise when experiments had observed a unique  $C_4$  symmetric magnetic order that preserves the tetragonal symmetry in a number of hole-doped FeSCs [20–25]. Such a  $C_4$  SDW state is characterized by bi-axial magnetic orders [26, 28–31], and the corresponding spin operator is given by  $S(\mathbf{r}) = M_X e^{i\mathbf{Q}_X\cdot\mathbf{r}} + M_Y e^{i\mathbf{Q}_Y\cdot\mathbf{r}}$

[31, 32]. It has been suggested that this double- $\mathbf{Q}$  magnetic state has two possible realizations [26–31]: a charge-spin density wave (CSDW) in which  $M_X$  and  $M_Y$  are collinear; a spin-vortex crystal (SVC) in which  $M_X$  and  $M_Y$  are orthogonal. Since the largest value of  $T_c$  of FeSCs is observed at the proximity of tetragonal  $C_4$  magnetic order [20, 21], there might exist a quantum critical point (QCP) at certain doping  $x_c$  in the superconducting (SC) dome [31]. After its discovery, the double- $\mathbf{Q}$  structured  $C_4$  SDW state has stimulated a variety of experimental [20–25] and theoretical works [26, 28–35].

In this paper, we consider the effects caused by the competition of superconductivity with both stripe-type  $C_2$  symmetric and  $C_4$  symmetric magnetic orders in a hole-doped FeSC  $\text{Ba}_{1-x}\text{K}_x\text{Fe}_2\text{As}_2$  [20–25]. Recently, Böhmer *et al.* [20] have experimentally investigated the global phase diagram of  $\text{Ba}_{1-x}\text{K}_x\text{Fe}_2\text{As}_2$ , and identified five distinct thermodynamically stable ordered phases, which are schematically shown in Fig. 1. One can see that the critical line for the nematic order displays a rather complicated dependence on doping  $x$  and temperature  $T$ : it decreases with growing  $x$  at high  $T$ , bends backwards to lower  $x$  slightly above  $T_c$ , and eventually exhibits a negative slope after penetrating into the SC dome. In the narrow doping region in which the nematic critical line has a positive slope,  $T_c$  is moderately suppressed. Close to the putative magnetic QCP, represented by  $x_2$  in Fig. 1, there appears on the phase diagram a region that manifests  $C_4$  symmetric SDW state, which occupies part of the usual  $C_2$  symmetric SDW phase and coexists with superconductivity below  $T_c$ . In principle, the experimentally observed  $C_4$  SDW state might be a CSDW or SVC type state, which needs to be clarified theoretically.

Instead of trying to explain the entire phase diagram observed in Ref. [20], we perform a more moderate task in this work. In particular, we will concentrate on the narrow doping region surrounding the magnetic QCP  $x_2$  inside the SC dome and endeavor to answer the following

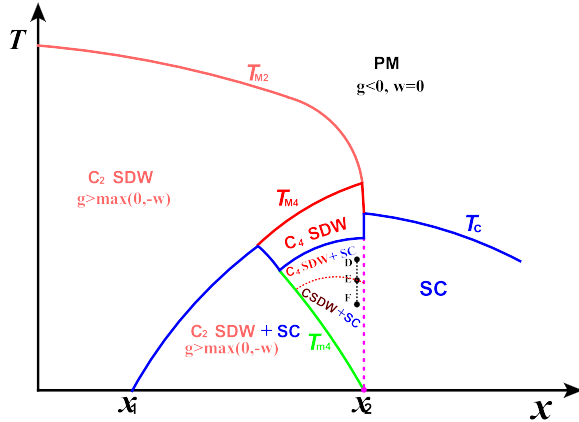


FIG. 1: (Color online) Schematic global phase diagram of  $\text{Ba}_{1-x}\text{K}_x\text{Fe}_2\text{As}_2$  on the  $(x, T)$  plane [20], with  $x_1$  and  $x_2$  being two QCPs.  $T_c$  is the critical line for SC phase transition.  $T_{M2}$  denotes the transition lines between paramagnetic (PM) and  $C_2$  magnetic phases.  $T_{M4}$  corresponds to the transition line from  $C_2$  magnetic to  $C_4$  magnetic phases in the absence of SC, whereas  $T_{m4}$  delineates the transition line from  $C_2$  magnetic to  $C_4$  magnetic phases inside the SC dome. The observed  $C_4$  symmetric SDW state could be either CSDW or SVC. Distinct phases are distinguished by different values of the model parameters [31, 32] defined in Eq. (4): (i)  $g < 0$  and  $w = 0$ , the system is in PM phase; (ii)  $g > \max(0, -w)$  represents the  $C_2$  symmetric SDW phase (with nematic order); (iii)  $C_4$  symmetric magnetic state is of SVC-type if  $g < 0$  and  $w > 0$ , and CSDW-type if  $g < -w$  and  $w < 0$ .

questions. How to determine whether the observed  $C_4$  magnetic state is of CSDW or SVC type? What is the scenario that leads to suppresses superconductivity near the magnetic QCP? Why does the nematic critical line display a negative, rather than positive, slope in the SC dome? We will address these issues by investigating the impact of order competition in the low- $T$  regime.

We study an effective field theory that can be used to describe the low-energy physics of  $\text{Ba}_{1-x}\text{K}_x\text{Fe}_2\text{As}_2$  and other analogous FeSCs [12, 18, 19, 27, 28, 55]. When the parameters used in this model take different values, the system might be in the paramagnetic state,  $C_4$  tetragonal SDW state, or  $C_2$  symmetric magnetic state. The fluctuations of the associated order parameters and the competition between distinct orders can qualitatively alter the magnitudes and even the sign of the model parameters, which would drive phase transitions and reshape the global phase diagram. After analyzing the competition between nematic and SC orders by means of renormalization group (RG) method, we find that the slope of nematic critical line is always negative in the SC dome. We also extract the  $T$ -dependence of superfluid density from RG results, which clearly shows that superconductivity is suppressed near magnetic QCP. Moreover, we infer from the RG results that, although CSDW and SVC state are both possible in the high- $T$  regime, the CSDW state is the only stable one in the low- $T$  regime, which provides a promising way to specify the true nature of the observed  $C_4$  symmetric SDW state.

The rest of paper is organized as follows. In Sec. II, we give the effective field theory for ordering competition and then derive the coupled flow equations of all the model parameters by performing perturbative RG calculations. In Sec. III, we numerically solve the equations and apply the RG solutions to understand several important features of the global phase diagram of  $\text{Ba}_{1-x}\text{K}_x\text{Fe}_2\text{As}_2$  observed in recent experiments. In Sec. IV, we present a brief summary of the results.

## II. EFFECTIVE THEORY AND RG ANALYSIS

Many of the basic properties of  $\text{Ba}_{1-x}\text{K}_x\text{Fe}_2\text{As}_2$  can be described by a three-band model that contains one hole pocket at the center of Brillouin zone  $\mathbf{Q}_\Gamma = (0, 0)$  and two electron pockets centered at two specific momenta  $\mathbf{Q}_X = (\pi, 0)$  and  $\mathbf{Q}_Y = (0, \pi)$  [12, 18, 19, 27, 28, 31, 32, 55]. The microscopic model is written as [12, 19]

$$H = \sum_{\mathbf{k}, i \in (X, Y, \Gamma)} \varepsilon_{\mathbf{k}, i} c_{\mathbf{k}\sigma, i}^\dagger c_{\mathbf{k}\sigma, i} + H_4, \quad (1)$$

with the interacting term  $H_4$  is given by

$$H_4 = \sum_{\mathbf{k}, i \in (X, Y)} \frac{U_3}{2} \left( c_{\mathbf{k}\alpha, \Gamma}^\dagger c_{\mathbf{k}\gamma, \Gamma}^\dagger c_{\mathbf{k}\delta, i} c_{\mathbf{k}\beta, i} + \text{h.c.} \right) \delta_{\alpha\beta} \delta_{\gamma\delta} + \sum_{\mathbf{k}, i \in (X, Y)} U_1 c_{\mathbf{k}\alpha, \Gamma}^\dagger c_{\mathbf{k}\gamma, i}^\dagger c_{\mathbf{k}\delta, i} c_{\mathbf{k}\beta, \Gamma} \delta_{\alpha\beta} \delta_{\gamma\delta}. \quad (2)$$

Here,  $U_1$  and  $U_3$  represent density-density interaction and the pair hoping interaction, respectively. They are responsible for the formation of superconductivity and SDW state [19, 36, 37]. The magnetic structure can be described by two order parameters  $\mathbf{M}_X$  and  $\mathbf{M}_Y$ , corresponding to the ordering vectors  $\mathbf{Q}_X = (\pi, 0)$  and  $\mathbf{Q}_Y = (0, \pi)$ , which are defined as  $\mathbf{M}_j = \sum_{\mathbf{k}} c_{\Gamma, \mathbf{k}\alpha}^\dagger \vec{\sigma}_{\alpha\beta} c_{j, \mathbf{k}+\mathbf{Q}_j, \beta}$  with  $j = X, Y$  [18, 19, 38–40]. Both the  $C_2$  and  $C_4$  symmetric magnetic orders are modeled by the following Ginzburg-Landau free energy [31, 32]

$$f[\mathbf{M}_X, \mathbf{M}_Y] = a_m (\mathbf{M}_X^2 + \mathbf{M}_Y^2) + \frac{u}{2} (\mathbf{M}_X^2 + \mathbf{M}_Y^2)^2 - \frac{g}{2} (\mathbf{M}_X^2 - \mathbf{M}_Y^2)^2 + 2w (\mathbf{M}_X \cdot \mathbf{M}_Y)^2.$$

As illustrated in Ref. [31], the term  $2w(\mathbf{M}_X \cdot \mathbf{M}_Y)^2$  can be rewritten by using an identity:

$$(\mathbf{M}_X \cdot \mathbf{M}_Y)^2 = \frac{1}{4} (\mathbf{M}_X^2 + \mathbf{M}_Y^2)^2 - \frac{1}{4} (\mathbf{M}_X^2 - \mathbf{M}_Y^2)^2 - (\mathbf{M}_X \times \mathbf{M}_Y)^2. \quad (3)$$

Upon carrying out a Hubbard-Stratonovich transformation followed by an integration over all the fermionic degrees of freedom, one can obtain an effective field theory [19, 31] for the interplay of SDW magnetic and SC orders

in the vicinity of magnetic QCP:

$$\begin{aligned} \mathcal{L} = & \frac{1}{2}(\partial_\mu M_X)^2 + \frac{1}{2}(\partial_\mu M_Y)^2 + a_m (M_X^2 + M_Y^2) \\ & + \frac{(u+w)}{2} (M_X^2 + M_Y^2)^2 - \frac{(g+w)}{2} (M_X^2 - M_Y^2)^2 \\ & + \partial_\mu \Delta^\dagger \partial_\mu \Delta + a_s \Delta^2(k) + \frac{u_s}{2} \Delta^4(k) + \frac{\varphi^2}{2w} + \mathcal{L}_A \\ & - 2\varphi M_X M_Y + \lambda(M_X^2 + M_Y^2) \Delta^2 + \lambda_{\Delta A} \Delta^2 A^2, \quad (4) \end{aligned}$$

where  $\Delta$  is the SC order parameter. Here we use a positive parameter  $\lambda$  to characterize the repulsive interaction (competition) between SC and magnetic orders. In order to evaluate the superfluid density, we have introduced a gauge potential  $\mathbf{A}$  to the effective theory via the standard minimal coupling [41] with  $\mathcal{L}_A = -\frac{1}{4}(\partial_\mu A_\nu - \partial_\nu A_\mu)^2$ . This model contains eight fundamental parameters  $a_m$ ,  $a_s$ ,  $u_s$ ,  $w$ ,  $u$ ,  $g$ ,  $\lambda$ , and  $\lambda_{\Delta A}$ , which are constants at the mean-field level, but all become cutoff dependent due to interactions.

The transition lines for SDW and SC orders are determined by taking  $a_m = 0$  and  $a_s = 0$  respectively. For  $s^{+-}$ -wave superconductors, we employ the relationship  $\Delta_\Gamma = -\sqrt{2}\Delta_{X,Y} = \Delta$  [8, 12, 19]. An Ising-type nematic order is induced by the magnetic order, and represented by a term of the form  $M_X^2 - M_Y^2$  [8, 12, 18]. The property of  $C_4$  magnetic order is determined by the parameter  $w$  [31, 32]. In the SC dome, the SC order parameter develops a nonzero mean value, i.e.,  $\langle \Delta \rangle = V_0 = \sqrt{-a_s/u_s}$  near the magnetic QCP  $x_2$ .

The effective model (4) displays different states when the model parameters take various values [31, 32]. (i) If  $g < 0$  and  $w = 0$ , the effective model is in paramagnetic (PM) phase; (ii) The case of  $g > \max(0, -w)$  corresponds to the  $C_2$  SDW phase (with nematic order); (iii) The  $C_4$  symmetric magnetic state is of SVC-type if  $g < 0$  and  $w > 0$ , and CSDW-type if  $g < -w$  and  $w < 0$ . Once some of these parameters are altered by external forces, such as doping, magnetic field, and pressure, the system would

undergo transitions between distinct phases. However, the quantum fluctuations of order parameters and the interaction between different order parameters can also lead to remarkable changes of model parameters, and as such drive phase transitions. In the next section, we will study the RG flows of these parameters and examine how they are influenced by order parameter fluctuation and ordering competition. The main results are schematically illuminated in Fig. 1 and the detailed derivations and discussions are given in the following.

To proceed, we perform a RG analysis of the effective theory (4). Our focus is on the behavior of the system at low  $T$  and in the vicinity of magnetic QCP. Within this region, the quantum fluctuations of SC order parameter can result in drastic effects even in the SC phase. For the complex SC order parameter  $\Delta(\mathbf{r})$ , there are two sorts of fluctuations [43–50], namely the phase fluctuation and amplitude fluctuation. The former fluctuation is gapless and corresponds to the Nambu-Goldstone mode induced by continuous gauge symmetry breaking. This mode does not play any role in the SC state because it is absorbed by the vector gauge boson via the Anderson-Higgs mechanism. The latter one, known as Higgs mode in a locally gauge invariant superconductor, is found by both theoretical and experimental works to result in observable effects [43–50], and hence should be seriously considered [51, 52]. In order to capture the quantum fluctuation of SC order parameter around its mean value  $\langle \Delta \rangle$ , we define two new fields  $h$  and  $\eta$  by [51, 52]

$$\Delta = V_0 + \frac{1}{\sqrt{2}}(h + i\eta), \quad (5)$$

where  $\langle h \rangle = \langle \eta \rangle = 0$ . The fields  $h$  and  $\eta$  represent the Higgs mode and Nambu-Goldstone mode, respectively. We substitute Eq. (5) into the effective Lagrangian density  $\mathcal{L}$  (4), and obtain the following new effective Lagrangian density:

$$\begin{aligned} \mathcal{L}_{\text{eff}} = & \frac{1}{2}(\partial_\mu M_X)^2 + \alpha_X M_X^2 + \frac{\beta_X}{2} M_X^4 + \frac{1}{2}(\partial_\mu M_Y)^2 + \alpha_Y M_Y^2 + \frac{\beta_Y}{2} M_Y^4 + \frac{1}{2}(\partial_\mu h)^2 + \alpha_h h^2 + \frac{\beta_h}{2} h^4 + \gamma_h h^3 \\ & + \left( \mathcal{L}_A + \frac{\alpha_A}{2} A^2 \right) + \alpha_\varphi \varphi^2 + \gamma_{\varphi XY} \varphi M_X M_Y + \gamma_{X^2 h} M_X^2 h + \gamma_{Y^2 h} M_Y^2 h + \gamma_{h A^2} h A^2 + \lambda_{X h} M_X^2 h^2 \\ & + \lambda_{Y h} M_Y^2 h^2 + \lambda_{X Y} M_X^2 M_Y^2 + \lambda_{h A} h^2 A^2. \quad (6) \end{aligned}$$

The gapless Nambu-Goldstone model  $\eta$  naturally disappears after invoking the Anderson-Higgs mechanism. However, the Higgs mode  $h$  remains in the above effective model, and couple directly to the magnetic order parameters  $M_{X,Y}$  and also to vector potential  $A$ . The originally massless gauge field  $A$  acquires a finite mass  $\alpha_A$  after absorbing  $\eta$ . Moreover, in the above Lagrangian density we have introduced a number of new parameters that are related to the model parameters defined in (4) by the following relations:

$$\begin{aligned} \alpha_X = \alpha_Y & \equiv a_m - \frac{\lambda a_s}{u_s}, \quad \alpha_A \equiv \frac{-2\lambda_{\Delta A} a_s}{u_s}, \quad \alpha_h \equiv -a_s, \quad \alpha_\varphi \equiv \frac{1}{2w}, \quad \beta_X = \beta_Y \equiv u - g, \quad \beta_h \equiv \frac{u_s}{4}, \\ \gamma_h & \equiv \frac{\sqrt{-2a_s u_s}}{2}, \quad \gamma_{h A^2} \equiv \sqrt{\frac{-2\lambda_{\Delta A}^2 a_s}{u_s}}, \quad \gamma_{\varphi XY} \equiv -2, \quad \gamma_{X^2 h} = \gamma_{Y^2 h} \equiv \sqrt{\frac{-2\lambda^2 a_s}{u_s}}, \\ \lambda_{X Y} & \equiv u + g + 2w, \quad \lambda_{h A} \equiv \frac{\lambda_{\Delta A}}{2}, \quad \lambda_{X h} = \lambda_{Y h} \equiv \frac{\lambda}{2}. \end{aligned} \quad (7)$$

Using these relations, we can derive the flow equations of fundamental parameters by calculating the effective parameters  $\alpha_X$ ,  $\alpha_h$ ,  $\alpha_\varphi$ ,  $\beta_X$ ,  $\beta_h$ ,  $\lambda_{XY}$ ,  $\lambda_{Xh}$ , and  $\lambda_{hA}$ . By performing perturbative expansion in powers of small coupling parameters [42] and utilizing  $\dot{u}$  to denote the derivative of  $u$  with respect to the varying length scale  $l$ , we arrive at the following flow equations with the help of the identities given by Eq. (7) [52]:

$$\begin{aligned}
\dot{a}_m &= 2 \left( a_m - \frac{\lambda a_s}{u_s} \right) + \frac{1}{4\pi^2} \left\{ \frac{\lambda}{2} (1 + 2a_s) + \frac{8\lambda^2 a_s^2}{u_s} + \left[ 1 - 2 \left( a_m - \frac{\lambda a_s}{u_s} \right) \right] \left[ 2(2u - g) + \frac{4\lambda^2 a_s}{u_s} \right] \right\} \\
&\quad + \left( \frac{\lambda}{u_s} \dot{a}_s + \frac{a_s}{u_s} \dot{\lambda} - \frac{a_s \lambda}{u_s^2} \dot{u}_s \right), \\
\dot{a}_s &= 2a_s - \frac{1}{12\pi^2} \left\{ \frac{27a_s u_s}{2} (1 + 4a_s) + \frac{12a_s \lambda^2}{u_s} \left[ 1 - 4 \left( a_m - \frac{a_s \lambda}{u_s} \right) \right] + 3\lambda \left[ 1 - 2 \left( a_m - \frac{a_s \lambda}{u_s} \right) \right] \right. \\
&\quad \left. + \frac{9u_s}{4} (1 + 2a_s) + 3\lambda_{\Delta A} \left( 1 + \frac{2a_s \lambda_{\Delta A}}{u_s} \right) + \frac{32a_s \lambda_{\Delta A}^2}{u_s} \left( 1 + \frac{4a_s \lambda_{\Delta A}}{u_s} \right) \right\}, \\
\dot{u}_s &= u_s + \frac{1}{\pi^2} \left\{ -\frac{9u_s^2}{4} (4a_s + 1) + 2\lambda^2 \left[ 4 \left( a_m - \frac{a_s \lambda}{u_s} \right) - 1 \right] + 54a_s u_s^2 (1 + 6a_s) - \frac{4\lambda_{\Delta A}^2}{3} \left( \frac{4a_s \lambda_{\Delta A}}{u_s} + 1 \right) \right. \\
&\quad \left. + \frac{32a_s \lambda^3}{u_s} \left( 1 + \frac{6a_s \lambda}{u_s} \right) + \frac{11072a_s \lambda_{\Delta A}^3}{35u_s} \left( 1 + \frac{6a_s \lambda_{\Delta A}}{u_s} \right) \right\}, \\
\dot{u} &= u + w + \frac{1}{2\pi^2} \left\{ [9(u - g)^2 + 3(u + g + 2w)(u - g) + 5(u + g + 2w)^2 + 12w(u - g)] \left[ 4 \left( a_m - \frac{a_s \lambda}{u_s} \right) - 1 \right] \right. \\
&\quad - \frac{3\lambda^2}{8} (4a_s + 1) + \frac{24a_s \lambda^2 (u - g)}{u_s} \left[ 1 - 2 \left( 2 \left( a_m - \frac{a_s \lambda}{u_s} \right) - a_s \right) \right] + 4w(u + g + 2w) \left[ 4 \left( a_m - \frac{a_s \lambda}{u_s} \right) - 1 \right] \\
&\quad \left. + \frac{8a_s \lambda^2 (u + g + 2w)}{u_s} \left[ 1 - 4 \left( a_m - \frac{a_s \lambda}{u_s} \right) + 2a_s \right] + \frac{4a_s \lambda^3}{u_s} \left[ 1 - 2 \left( a_m - \frac{a_s \lambda}{u_s} \right) + 4a_s \right] \right\} - \dot{w}, \\
\dot{g} &= g + w - \frac{1}{2\pi^2} \left\{ [9(u - g)^2 - 3(u + g + 2w)(u - g) - 3(u + g + 2w)^2 - 12w(u - g)] \left[ 4 \left( a_m - \frac{a_s \lambda}{u_s} \right) - 1 \right] \right. \\
&\quad - \frac{\lambda^2}{8} (4a_s + 1) + \frac{24a_s \lambda^2 (u - g)}{u_s} \left[ 1 - 2 \left( 2 \left( a_m - \frac{a_s \lambda}{u_s} \right) - a_s \right) \right] + 4w(u + g + 2w) \left[ 4 \left( a_m - \frac{a_s \lambda}{u_s} \right) - 1 \right] \\
&\quad \left. - \frac{8a_s \lambda^2 (u + g + 2w)}{u_s} \left[ 1 - 4 \left( a_m - \frac{a_s \lambda}{u_s} \right) + 2a_s \right] + \frac{4a_s \lambda^3}{u_s} \left[ 1 - 2 \left( a_m - \frac{a_s \lambda}{u_s} \right) + 4a_s \right] \right\} - \dot{w}, \\
\dot{\lambda} &= \lambda + \frac{1}{\pi^2} \left\{ \frac{4a_s \lambda^3}{u_s} \left[ 1 - 4 \left( a_m - \frac{a_s \lambda}{u_s} \right) + 2a_s \right] + \lambda(2u - g + 3w) \left[ 4 \left( a_m - \frac{a_s \lambda}{u_s} \right) - 1 \right] \right. \\
&\quad + \frac{16a_s \lambda^2 (2u - g + w)}{u_s} \left[ 1 - 6 \left( a_m - \frac{a_s \lambda}{u_s} \right) \right] + 6a_s \lambda^2 \left[ 1 - 2 \left( a_m - \frac{a_s \lambda}{u_s} \right) + 4a_s \right] \\
&\quad \left. - \frac{3u_s \lambda}{8} (4a_s + 1) + 2\lambda^2 \left[ 2 \left( a_m - \frac{a_s \lambda}{u_s} \right) - 2a_s - 1 \right] + 9a_s u_s \lambda (1 + 6a_s) \right\}, \\
\dot{\lambda}_{\Delta A} &= \lambda_{\Delta A} + \frac{1}{3\pi^2} \left\{ 27a_s u_s \lambda_{\Delta A} (1 + 6a_s) + \frac{4\lambda_{\Delta A}^2 (16a_s \lambda_{\Delta A} - 3u_s)}{u_s} \left[ 1 + 2a_s \left( 1 + \frac{2\lambda_{\Delta A}}{u_s} \right) \right] \right. \\
&\quad \left. - \frac{9u_s \lambda_{\Delta A}}{8} (4a_s + 1) + 36a_s \lambda_{\Delta A}^2 \left[ 1 + 2a_s \left( 2 + \frac{\lambda_{\Delta A}}{u_s} \right) \right] \right\}, \\
\dot{w} &= \frac{w^2}{\pi^2} \left[ 1 - 4 \left( a_m - \frac{\lambda a_s}{u_s} \right) \right].
\end{aligned} \tag{8}$$

### III. COMPARISON WITH EXPERIMENTS

In this section, we will compare the RG results with recent experiments. We first numerically solve the self-consistently coupled RG equations, and then manage to understand a number of important features observed by Böhmer *et al.* in  $\text{Ba}_{1-x}\text{K}_x\text{Fe}_2\text{As}_2$  [20]. We are particularly interested in the doping dependence of nematic critical line in the SC dome, the suppression of superconductivity observed at the magnetic QCP, and the nature of the observed  $C_4$  symmetric magnetic order, which will

be studied one by one based on the RG solutions.

As can be seen from the phase diagram presented in Fig. 1, the magnetic and SC orders are assumed to coexist over a finite region, with  $x_2$  being the magnetic QCP. Such a coexistence can be realized if the bare values of model parameters satisfy the constraint [19, 53–57]  $\lambda < \sqrt{u_s[(u + w) - (g + w)]} = \sqrt{u_s(u - g)}$ . For simplicity, we will only consider the low- $T$  region in the close vicinity of the magnetic QCP inside the SC dome. In addition, the external field  $A$  is assumed to be weak, but the basic conclusion does not depend on this assumption.

### A. Slope of nematic critical line in SC dome

The nematic line is not shown apparently in Fig. 1. However, the  $C_2$  magnetic phase is always accompanied (even preempted) by a nematic phase with a critical temperature  $T_n$  higher than that of  $C_2$  magnetic order [6, 8, 10, 12, 19]. Therefore,  $T_{m4}$  is also a nematic critical line.

A known fact is that a long-range order can always be destroyed by thermal fluctuation at sufficiently high  $T$ . In a system containing two or more distinct orders, the competition between these orders might destroy some specific order at very low  $T$ . As a result, the critical line on the  $(x, T)$  phase diagram for this specific order has a positive slope in the low- $T$  region, which is often called backbending behavior. Interestingly, such backbending behavior has been observed in some high- $T_c$  cuprate superconductor [58–60] and FeSCs [61]. In cuprate  $\text{Bi}_2\text{Sr}_2\text{CaCu}_2\text{O}_{8+\delta}$ , a pseudogap exists above  $T_c$  on the  $(x, T)$  phase diagram. This pseudogap decreases rapidly with growing doping  $x$ , so its critical line exhibits a negative slope above  $T_c$ . However, after entering into the SC dome, the critical line for pseudogap was found to bend backwards to lower doping, and thus displays a positive slope in the low- $T$  region [58–60]. A similar behavior was also observed in  $\text{Ba}(\text{Fe}_{1-x}\text{Co}_x)_2\text{As}_2$  by Nandi *et al.* [61]. In this case, it is the nematic order that is in strong competition with SC order. The nematic critical line has a negative slope on  $(x, T)$  phase diagram above  $T_c$ , but displays a positive slope below  $T_c$  [61]. A common feature observed in these two compounds is that the critical line for the order competing with superconductivity has a positive slope in the low- $T$  region. While a convincing theoretic explanation for the backbending of pseudogap critical line in  $\text{Bi}_2\text{Sr}_2\text{CaCu}_2\text{O}_{8+\delta}$  is lacking, a recent RG work reproduced the backbending of nematic critical line by studying the competition between nematic and SC orders in  $\text{Ba}(\text{Fe}_{1-x}\text{Co}_x)_2\text{As}_2$  [62]. Different from  $\text{Ba}(\text{Fe}_{1-x}\text{Co}_x)_2\text{As}_2$ , the nematic critical line has a negative slope in the SC dome of  $\text{Ba}_{1-x}\text{K}_x\text{Fe}_2\text{As}_2$  [20] despite the presence of ordering competition.

In  $\text{Ba}(\text{Fe}_{1-x}\text{Co}_x)_2\text{As}_2$ , there is only  $C_2$  symmetric magnetic order, induced by a stripe-type SDW state. As discussed in Ref. [19], the existence of nematic order is tuned by the quadratic term  $-g(M_X^2 - M_Y^2)^2$ . The system can stay either in the PM phase, or in one of the  $M_X$  and  $M_Y$  magnetically ordered phases. The former case corresponds to a state in which  $g < 0$  and no nematic order exists. In the latter case,  $g > 0$  and hence the system exhibits a nematic order. Both of these two possibilities can be realized at low  $T$ . When the competition between nematic and SC orders is sufficiently strong, it is in principle possible for the nematic order to be suppressed in the low- $T$  region, leading to a positive slope of nematic critical line in the SC dome [62].

We now use the RG solutions to judge whether the nematic critical line has a positive or negative slope in the SC dome of  $\text{Ba}_{1-x}\text{K}_x\text{Fe}_2\text{As}_2$ . In the effective field

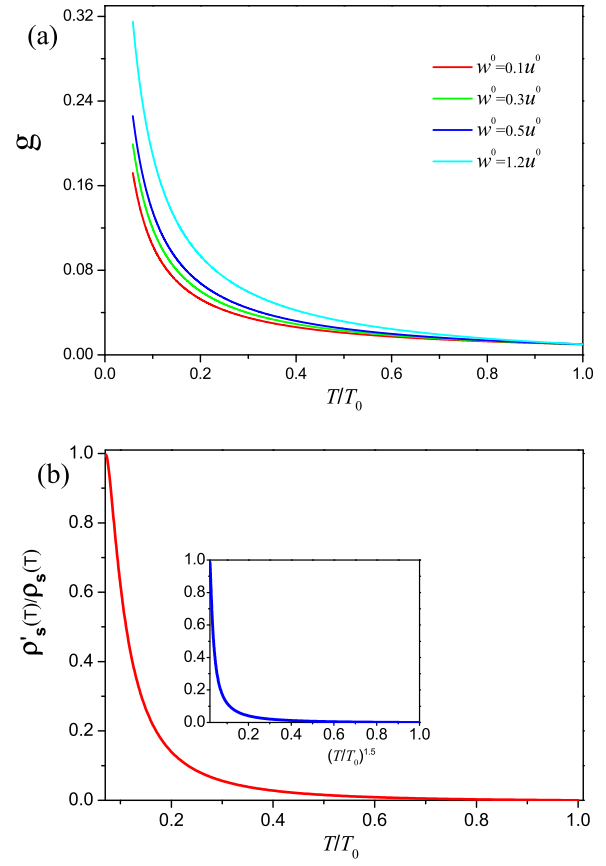


FIG. 2: (Color online) (a)  $T$ -dependence of  $g$  at several different values of  $w_0$  (calculations found that  $g$  does not become negative as  $T$  decreases). (b)  $T$ -dependence of the ratio  $\rho'_s(T)/\rho_s(T)$ .

model given by Eq. (4), the relation between  $g$  and  $w$  determines whether the nematic order is present or not. As pointed out previously in Refs. [10, 18, 62], when  $g > \max(0, -w)$ , only one of the two order parameters  $M_X$  and  $M_Y$  develops a finite mean value due to tetragonal symmetry breaking, which is a clear signature for the existence of a nematic order. On the other hand, we have  $\langle M_X \rangle = \langle M_Y \rangle$  if  $g < \max(0, -w)$ , which implies the absence of nematic order [10, 18, 62]. This property will be used to judge whether the nematic critical line bends back. Now imagine the nematic critical line has a positive slope in the SC dome, namely the line bends backwards to smaller  $x$  as  $T$  is lowered. If we start from a state with nematic and SC orders coexisting at certain finite  $T$  above the nematic critical line, the nematic order would be entirely destroyed as  $T$  decreases across the critical line. In this case, we have  $g > \max(0, -w)$  above the nematic critical line and  $g < \max(0, -w)$  below it. In contrast, if the nematic critical line has a negative slope in the SC dome and does not exhibit backbending behavior, the inequality  $g > \max(0, -w)$  is always satisfied

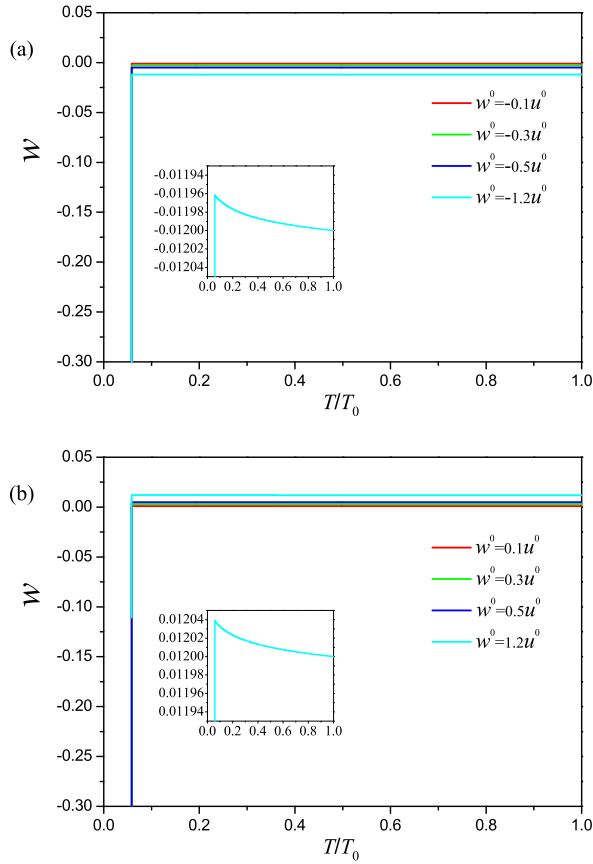


FIG. 3: (Color online)  $T$ -dependence of parameter  $w$  obtained at given bare values of dimensionless parameters:  $a_s^0 = -0.001$ ,  $u_s^0 = 0.05$ ,  $u^0 = 0.01$ ,  $g^0 = -0.01$ ,  $\lambda^0 = 0.01$ , and  $\lambda_{\Delta A}^0 = 1.0 \times 10^{-8}$ . The main conclusion is independent of these bare values. The parameter  $w$  is not very sensitive to the change of  $T$ , so we provide two insets to show more clearly how  $w$  varies as  $T$  is decreasing. (a) Starting point is CSDW-type  $C_4$  state with  $w^0 < 0$ ; (b) Starting point is SVC-type  $C_4$  state with  $w^0 > 0$ .

as  $T$  decreases down to zero.

To examine how the relation between  $g$  and  $w$  varies with decreasing  $T$ , we solve the RG equations and obtain its dependence on the tuning length scale  $l$ . For concreteness, we choose the following bare values of models parameters:  $a_s^0 = -0.001$ ,  $u^0 = 0.05$ ,  $u_s^0 = 0.01$ ,  $g^0 = 0.01$ ,  $\lambda^0 = 0.01$ ,  $\lambda_{\Delta A}^0 = 1.0 \times 10^{-8}$ . We take several different values of  $w^0$ :  $w^0 = 0.1u^0, 0.3u^0, 0.5u^0$ , and  $1.2u^0$ . The  $l$ -dependence of these parameters can be easily converted to a  $T$ -dependence by utilizing the transformation [62, 63]  $T = T_0 e^{-l}$  with  $T_0$  being certain specific temperature. The numerical results are presented in Fig. 2 (a). As  $T$  is lowered, we find that the inequality  $g > \max(0, -w)$  is always fulfilled. This result clearly indicates that the nematic critical line has a negative slope in the SC dome and never bends backwards, which is well consistent with the recently observed phase diagram [20].

## B. Suppression of superconductivity due to ordering competition

We now verify whether superconductivity is suppressed by ordering competition in the vicinity of the magnetic QCP. To this end, we will compute the superfluid density after taking into account the ordering competition among nematic ( $C_2$  SDW),  $C_4$  SDW and SC orders. The superfluid density  $\rho_s$  can be evaluated by virtue of the formula  $\rho_s \propto \alpha_A$ , where  $\alpha_A$  is the mass for vector potential  $\mathbf{A}$  generated via Anderson-Higgs mechanism [41].

The  $T$ -dependence of superfluid density  $\rho_s(T)$  is computed from the  $l$ -dependence of parameter  $\alpha_A \equiv \alpha_A(l)$  [63, 67], which is extracted from the coupled flow equation (8) and hence captures the ordering competition. To make a quantitative analysis, we introduce a ratio  $\rho'_s(T)/\rho_s(T)$ , where  $\rho'_s(T)$  is the superfluid density that includes ordering competitions and  $\rho_s(T)$  is the one in a pure SC state. As can be seen from Fig. 2(b), this ratio vanishes at some temperature smaller than the pure case, which is a clear signature that superconductivity is suppressed by ordering competition in the vicinity of QCP  $x_2$ . In particular, the SC transition line, represented by  $T_c$ , becomes lower due to ordering competition. This result is in qualitative agreement with recent experiment [20], in which a considerable drop of  $T_c$  is observed near the putative magnetic QCP.

## C. $C_4$ symmetric magnetic order

We finally turn to analyze the property of  $C_4$  symmetric magnetic state. To uncover the effects caused by ordering competition, we consider the evolution of the system along the route  $D \rightarrow E \rightarrow F$ , shown in Fig. 1, and examine how  $g$  and  $w$  vary along this route.

Eq. (4) clearly shows that  $w$  is associated with the quadratic term of  $C_4$  SDW order parameter [31, 32]. In analogy to the nematic transition, the sign of  $w$  determines which sort of  $C_4$  SDW order, either SVC or CSDW, is realized [10, 18, 31, 32, 62]. In particular, a  $C_4$  SVC order is generated for  $g < 0$  and  $w > 0$ , whereas  $g < -w$  and  $w < 0$  implies the occurrence of a  $C_4$  CSDW order [10, 18, 31, 32, 62]. By paralleling the analysis made in the case of nematic critical line, we convert the  $l$ -dependence of  $w$  using the transformation  $T = T_0 e^{-l}$  [63, 67]. If one assumes that  $w$  is negative at the starting point  $D$ , which amounts to supposing the system is in the CSDW-type  $C_4$  magnetic state, it remains negative as  $T$  decreases down to the  $F$  point, as can be clearly seen from Fig. 3(a). This result implies the stability of the CSDW state in the low- $T$  region. On the other hand, if one starts from a positive  $w$ , corresponding to a SVC-type  $C_4$  magnetic state, we show in Fig. 3(b) that  $w$  eventually becomes negative at some critical  $T$ , which can be identified as the  $E$  point. We thus infer that the SVC state is unstable in the low- $T$  region, where CSDW state is more favorable than SVC

state.

We conclude from the above analysis that, although in principle either SVC or CSDW type  $C_4$  state could be realized in the high- $T$  region, the CSDW-type  $C_4$  state is the only stable one in the low- $T$  region. In a recent work, Christensen *et al.* [68] have suggested the spin-orbit coupling gives rises to the CSDW-type  $C_4$  SDW. Additional, Hoyer *et al.* [32] have studied the disorder effects and demonstrated that impurity scattering favors CSDW over SVC. Here, we provide a different approach to determine the nature of  $C_4$  symmetric magnetic order. Moreover, the sudden drop of  $w$  at certain critical energy scale usually indicates the happening of a first-order transition, which is qualitatively consistent with recent experiments [20].

#### IV. SUMMARY

In summary, we have studied the impact of the competition between superconductivity and  $C_2$  and  $C_4$  symmetric magnetic orders in a hole-doped FeSC  $\text{Ba}_{1-x}\text{K}_x\text{Fe}_2\text{As}_2$ . After performing a detailed RG analysis within an effective field theory, we have reproduced a number of interesting features of the global phase diagram. In particular, our RG analysis have showed that the order parameter fluctuation and ordering competition lead to moderate suppression of superconductivity near the magnetic QCP, maintain the negative slope of nematic critical line in the SC dome, and also select out the CSDW-type  $C_4$  magnetic order as the more stable state than a SVC-type  $C_4$  magnetic order in the low- $T$  regime. All these theoretic results are well consistent

with the recent experiments of Ref. [20], and schematically summarized in Fig. 1.

Our RG calculations are confined to the small region surrounding the magnetic QCP in the SC dome. To gain a better knowledge of the entire phase diagram, it is necessary to consider the non-SC phase above  $T_c$ . A salient feature observed in Ref. [20] is the backbending behavior of a critical line between nematic ( $C_2$  SDW) to pure  $C_4$  SDW orders, namely  $T_{M4}$ , which turns out to be induced by the emergence of  $C_4$  symmetric magnetic order. To account for this feature, one might need to study the interaction between elementary fermionic excitations and magnetic orders ( $C_2$  or  $C_4$ ), which are left for future research.

#### V. ACKNOWLEDGEMENTS

J.W. and G.Z.L are financially supported by the National Natural Science Foundation of China under Grants 11274286, 11574285, and 11504360. J.W. is also supported by the China Postdoctoral Science Foundation under Grants 2015T80655 and 2014M560510, the Fundamental Research Funds for the Central Universities (P. R. China) under Grant WK2030040074, and the Program of Study Abroad for Young Scholar sponsored by CSC (China Scholarship Council). D.V.E. and J.v.d.B would like to acknowledge the financial support provided by the German Research Foundation (Deutsche Forschungsgemeinschaft) through priority program SPP 1458. J.v.d.B is also supported by SFB 1143 of the Deutsche Forschungsgemeinschaft.

---

[1] D. S. Inosov, J. T. Park, P. Bourges, D. L. Sun, Y. Sidis, A. Schneidewind, K. Hradil, D. Haug, C. T. Lin, B. Keimer and V. Hinkov, *Nat. Phys.* **6**, 178 (2009).

[2] J. Paglione and R. L. Greene, *Nat. Phys.* **6**, 645 (2010).

[3] G. R. Stewart, *Rev. Mod. Phys.* **83**, 1589 (2011).

[4] I. R. Fisher, L. Degiorgi, and Z. X. Shen, *Rep. Prog. Phys.* **74**, 124506 (2011).

[5] P. J. Hirschfeld, M. M. Korshunov, and I. I. Mazin, *Rep. Prog. Phys.* **74**, 124508 (2011).

[6] D. N. Basov and A. V. Chubukov, *Nat. Phys.* **7**, 272 (2011).

[7] P. Dai, J. Hu, and E. Dagotto, *Nat. Phys.* **8**, 709 (2012).

[8] A. V. Chubukov, *Annu. Rev. Condens. Matter Phys.* **3**, 57 (2012).

[9] E. Dagotto, *Rev. Mod. Phys.* **85**, 849 (2013).

[10] R. M. Fernandes, A. V. Chubukov, and J. Schmalian, *Nat. Phys.* **10**, 97 (2014).

[11] P. C. Dai, *Rev. Mod. Phys.* **87**, 855 (2015).

[12] R. M. Fernandes and A. V. Chubukov, arXiv: 1607.00865v1 (2016).

[13] M. G. Kim, R. M. Fernandes, A. Kreyssig, J. W. Kim, A. Thaler, S. L. Bud'ko, P. C. Canfield, R. J. McQueeney, J. Schmalian, and A. I. Goldman. *Phys. Rev. B* **83**, 134522 (2011).

[14] C. R. Rotundu and R. J. Birgeneau, *Phys. Rev. B* **84**, 092501 (2011).

[15] S. Avci, O. Chmaissem, D. Y. Chung, S. Rosenkranz, E. A. Goremychkin, J. P. Castellan, I. S. Todorov, J. A. Schlueter, H. Claus, A. Daoud-Aladine, D. D. Khalyavin, M. G. Kanatzidis, and R. Osborn, *Phys. Rev. B* **85**, 184507 (2012).

[16] S. Kasahara, H. J. Shi, K. Hashimoto, S. Tonegawa, Y. Mizukami, T. Shibauchi, K. Sugimoto, T. Fukuda, T. Terashima, A. H. Nevidomskyy and Y. Matsuda, *Nature* **486**, 382 (2012).

[17] R. Zhou, Z. Li, J. Yang, D. L. Sun, C. T. Lin, and G.-Q Zheng, *Nature Comm.* **4**, 2265 (2013).

[18] R. M. Fernandes, A. V. Chubukov, J. Knolle, I. Eremin, and J. Schmalian, *Phys. Rev. B* **85**, 024534 (2012).

[19] R. M. Fernandes, S. Maiti, P. Wölfe, and A. V. Chubukov, *Phys. Rev. Lett.* **111**, 057001 (2013).

[20] A. E. Böhmer, F. Hardy, L. Wang, T. Wolf, P. Schweiss, and C. Meingast, *Nat. Commun.* **6**, 7911 (2015).

[21] S. Avci, O. Chmaissem, J. M. Allred, S. Rosenkranz, I. Eremin, A. V. Chubukov, D. E. Bulgaris, D. Y. Chung, M. G. Kanatzidis, J.-P. Castellan, J. A. Schlueter, H.

Claus, D. D. Khalyavin, P. Manuel, A. Daoud-Aladine, and R. Osborn, *Nature Commun.* **5**, 3845 (2014).

[22] M. G. Kim, A. Kreyssig, A. Thaler, D. K. Pratt, W. Tian, J. L. Zarestky, M. A. Green, S. L. Bud'ko, P. C. Canfield, R. J. McQueeney, and A. I. Goldman, *Phys. Rev. B* **82**, 220503(R) (2010).

[23] E. Hassinger, G. Gredat, F. Valade, S. René de Cotret, A. Juneau-Fecteau, J.-Ph. Reid, H. Kim, M. A. Tanatar, R. Prozorov, B. Shen, H.-H. Wen, N. DoironLeyraud, and Louis Taillefer, *Phys. Rev. B* **86**, 140502 (2012).

[24] J. M. Allred, S. Avci, D. Y. Chung, H. Claus, D. D. Khalyavin, P. Manuel, K. M. Taddei, M. G. Kanatzidis, S. Rosenkranz, R. Osborn, and O. Chmaissem, *Phys. Rev. B* **92**, 094515 (2015).

[25] J. M. Allred, K. M. Taddei, D. E. Bugaris, M. J. Krogstad, S. H. Lapidus, D. Y. Chung, H. Claus, M. G. Kanatzidis, D. E. Brown, J. Kang, R. M. Fernandes, I. Eremin, S. Rosenkranz, O. Chmaissem, and R. Osborn, *Nature Phys.* **10**, 1038 (2016).

[26] J. Lorenzana, G. Seibold, C. Ortix, and M. Grilli, *Phys. Rev. Lett.* **101**, 186402 (2008).

[27] J. Knolle, I. Eremin, A. V. Chubukov, and R. Moessner, *Phys. Rev. B* **81**, 140506(R) (2010).

[28] I. Eremin and A. V. Chubukov, *Phys. Rev. B* **81**, 024511 (2010).

[29] P. M. R. Brydon, J. Schmiedt, and C. Timm, *Phys. Rev. B* **84**, 214510 (2010).

[30] G. Giovannetti, C. Ortix, M. Marsman, M. Capone, J. Brink and J. Lorenzana, *Nat. Comm.* **2**, 398 (2011).

[31] R. M. Fernandes, S. A. Kivelson, and E. Berg, *Phys. Rev. B* **93**, 014511 (2016)

[32] M. Hoyer, R. M. Fernandes, A. Levchenko, and J. Schmalian, *Phys. Rev. B* **93**, 144414 (2016)

[33] D. D. Scherer, I. Eremin, and B. M. Andersen, arXiv:1608.03493v1 (2016).

[34] J. Kang and Z. Tesanovic, *Phys. Rev. B* **83**, 020505 (2011).

[35] M. N. Gastiasoro and B. M. Andersen, *Phys. Rev. Lett.* **113**, 067002 (2014).

[36] A. V. Chubukov, D. V. Efremov, and I. Eremin, *Phys. Rev. B* **78**, 134512 (2008).

[37] S. Maiti and A. V. Chubukov, *Phys. Rev. B* **82**, 214515 (2010).

[38] C. Fang, H. Yao, W.-F. Tsai, J. P. Hu, and S.A. Kivelson, *Phys. Rev. B* **77**, 224509 (2008).

[39] C. Xu, M. Muller, and S. Sachdev, *Phys. Rev. B* **78**, 020501(R) (2008).

[40] R. M. Fernandes, L. H. VanBebber, S. Bhattacharya, P. Chandra, V. Keppens, D. Mandrus, M. A. McGuire, B. C. Sales, A. S. Sefat, and J. Schmalian, *Phys. Rev. Lett.* **105**, 157003 (2010).

[41] B. I. Halperin, T. C. Lubensky, and S.-K. Ma, *Phys. Rev. Lett.* **32**, 292 (1974).

[42] R. Shankar, *Rev. Mod. Phys.* **66**, 129 (1994).

[43] C. M. Varma, *J. Low Temp. Phys.* **126**, 901 (2002).

[44] W. Zwerger, *Phys. Rev. Lett.* **92**, 027203 (2004).

[45] D. Podolsky, A. Auerbach, and D. P. Arovas, *Phys. Rev. B* **84**, 174522 (2011).

[46] D. Podolsky and S. Sachdev, *Phys. Rev. B* **86**, 054508 (2012).

[47] L. Pollet and N. Prokof'ev, *Phys. Rev. Lett.* **109**, 010401 (2012).

[48] M. Endres, T. Fukuhara, D. Pekker, M. Cheneau, P. Schaub, C. Gross, E. Demler, S. Kuhr, and I. Bloch, *Nature* **487**, 454 (2012).

[49] Y. Barlas and C. M. Varma, *Phys. Rev. B* **87**, 054503 (2013).

[50] D. Pekker and C. M. Varma, *Annu. Rev. Condens. Matter Phys.* **6**, 269 (2015).

[51] H. Kleinert and F. S. Nogueira, *Nucl. Phys. B* **651**, 361 (2003).

[52] J. Wang and G.-Z. Liu, *Phys. Rev. D* **90**, 125015 (2014).

[53] J.-H. She, J. Zaanen, A. R. Bishop, and A. V. Balatsky, *Phys. Rev. B* **82**, 165128 (2010).

[54] A. B. Vorontsov, M. G. Vavilov, and A. V. Chubukov, *Phys. Rev. B* **79**, 060508(R) (2009); A. B. Vorontsov, M. G. Vavilov, and A. V. Chubukov, *Phys. Rev. B* **81**, 174538 (2010).

[55] R. M. Fernandes, D. K. Pratt, W. Tian, J. Zarestky, A. Kreyssig, S. Nandi, M. G. Kim, A. Thaler, N. Ni, P. C. Canfield, R. J. McQueeney, J. Schmalian, and A. I. Goldman, *Phys. Rev. B* **81**, 140501(R) (2010).

[56] R. M. Fernandes and J. Schmalian, *Phys. Rev. B* **82**, 014521 (2010).

[57] J. Wang and G.-Z. Liu, *New J. Phys.* **15**, 073039 (2013).

[58] I. M. Vishik, M. Hashimoto, R.-H. He, W.-S. Lee, F. Schmitt, D. Lu, R. G. Moore, C. Zhang, W. Meevasana, T. Sasagawa, S. Uchida, K. Fujita, S. Ishida, M. Ishikado, Y. Yoshida, H. Eisaki, Z. Hussain, T. P. Devereaux, and Z.-X. Shen, *Proc. Natl. Acad. Sci. USA* **109**, 18332 (2012).

[59] M. Hashimoto, E. A. Nowadnick, R.-H. He, I. M. Vishik, B. Moritz, Y. He, K. Tanaka, R. G. Moore, D. Lu, Y. Yoshida, M. Ishikado, T. Sasagawa, K. Fujita, S. Ishida, S. Uchida, H. Eisaki, Z. Hussain, T. P. Devereaux, and Z.-X. Shen, *Nat. Mat.* **14**, 37 (2015).

[60] M. Hashimoto, I. M. Vishik, R.-H. He, T. P. Devereaux, and Z.-X. Shen, *Nat. Phys.* **10**, 483 (2014).

[61] S. Nandi, M. G. Kim, A. Kreyssig, R. M. Fernandes, D. K. Pratt, A. Thaler, N. Ni, S. L. Bud'ko, P. C. Canfield, J. Schmalian, R. J. McQueeney, and A. I. Goldman, *Phys. Rev. Lett.* **104**, 057006 (2010).

[62] J. Wang and G.-Z. Liu, *Phys. Rev. B* **92**, 184510 (2015).

[63] J.-H. She, M. J. Lawler, and E.-A. Kim, *Phys. Rev. B* **92**, 035112 (2015).

[64] D. K. Pratt, W. Tian, A. Kreyssig, J. L. Zarestky, S. Nandi, N. Ni, S. L. Bud'ko, P. C. Canfield, A. I. Goldman, and R. J. McQueeney, *Phys. Rev. Lett.* **103**, 087001 (2009).

[65] A. D. Christianson, M. D. Lumsden, S. E. Nagler, G. J. MacDougall, M. A. McGuire, A. S. Sefat, R. Jin, B. C. Sales, and D. Mandrus, *Phys. Rev. Lett.* **103**, 087002 (2009).

[66] A. Kreyssig, M. G. Kim, S. Nandi, D. K. Pratt, W. Tian, J. L. Zarestky, N. Ni, A. Thaler, S. L. Bud'ko, P. C. Canfield, R. J. McQueeney, and A. I. Goldman, *Phys. Rev. B* **81**, 134512 (2010).

[67] Y. Huh and S. Sachdev, *Phys. Rev. B* **78**, 064512 (2008).

[68] M. H. Christensen, J. Kang, B. M. Andersen, I. Eremin, and R. M. Fernandes, *Phys. Rev. B* **92**, 214509 (2015).